

# EyeLight: Light-and-shadow-based Occupancy Estimation and Room Activity Recognition

Viet Nguyen\*, Mohamed Ibrahim\*, Siddharth Rupavatharam, Minitha Jawahar,  
Marco Gruteser, Richard Howard  
WINLAB, Rutgers University.

{vietnh, mibrahim, gruteser, reh}@winlab.rutgers.edu, {siddharth.r, minitha.jawahar}.rutgers.edu

\* The first two authors are co-primary student authors.

**Abstract**—This paper explores the feasibility of localizing and detecting activities of building occupants using visible light sensing across a mesh of light bulbs. Existing Visible Light activity sensing (VLS) techniques require either light sensors to be deployed on the floor or a person to carry a device. Our approach integrates photosensors with light bulbs and exploits the light reflected off the floor to achieve an entirely device-free and light source based system. This forms a mesh of virtual light barriers across networked lights to track shadows cast by occupants. The design employs a synchronization circuit that implements a time division signaling scheme to differentiate between light sources and a sensitive sensing circuit to detect small changes in weak reflections. Sensor readings are fed into indoor supervised tracking algorithms as well as occupancy and activity recognition classifiers. Our prototype uses modified off-the-shelf LED flood light bulbs and is installed in a typical office conference room. We evaluate the performance of our system in terms of localization, occupancy estimation and activity classification, and find a 0.89m median localization error as well as 93.7% and 93.78% occupancy and activity classification accuracy, respectively.

## I. INTRODUCTION

Building-wide occupancy detection and activity sensing promises to enable a new class of applications across smart homes, elderly care, and retail marketing. In smart homes, for example, it could enhance control of lighting, heating, ventilation, and air conditioning based on sensed and predicted activities across rooms. Useful information ranges from basic occupancy and movement tracking to activity inference (e.g., sleeping, cooking, eating, watching TV or media). In elderly care, activity sensing allows quick detection of emergencies or changes in routine. In stores and showrooms, foot traffic statistics for individual aisles or product display areas are invaluable for ad placement and arranging products.

**Existing occupancy sensing technologies.** These activities are currently detected by a number of dedicated sensing systems, with Infrared (IR) motion sensing being especially prevalent. Passive or Pyroelectric Infrared (PIR) sensors detect the radiated IR energy from humans and animals [26]. However, PIR sensors require line-of-sight coverage, which increases the number of required sensors to cover a certain area. For example, previous work [24] required one sensor per 4 meter square area. PIR sensors are also sensitive to other heat sources (e.g., hot appliances, sunlight and open window), and they are designed to detect movements, not presence,

which limits its tracking of stationary users. For more fine-grained detection in a small area, light barriers detect motion when transmission between an IR transmitter and receiver is obstructed. Other device-free solutions have relied on cameras [14]. Although they are effective and ubiquitous in public places, cameras raise privacy issues, especially in residential areas. More recently, Wifi-based activity sensing (e.g., [23]), has been proposed, which generally achieves large coverage at lower accuracy and faces more challenges to scale to buildings with many occupants. Besides such device-free sensing, other approaches leverage user devices like smart watches and smart phones (e.g., [12]). The disadvantage of these approaches is that users need to continuously carry, wear, and usually charge them.

More recently, fine-grained localization and activity sensing using visible light has been investigated. Current VLS work mainly uses active techniques (users are required to carry sensors or devices) and focuses on line-of-sight communication between transmitter and receiver [15], [27]. Among passive (device-free) techniques, LiSense [16] demonstrates fine-grained gesture and human skeleton reconstruction using visible light sensing but requires deploying photodiodes on the floor to obtain line-of-sight links with the transmitters. CeilingSee [25] converts ceiling mounted LED luminaries to act as photosensors, to infer indoor occupancy, but requires dense deployment (1.25m between nearby pair) of LED luminaries because of reduced sensitivity of LEDs acting like photosensors compared to dedicated photosensors. None of these technologies can therefore provide device-free occupancy sensing beyond line of sight, which would enable building scale fine-grained activity sensing with lower deployment overhead (i.e. using fewer sensors).

**EyeLight Approach.** We introduce EyeLight, a device-free occupancy detection and activity sensing system exploiting opportunistic, indirect light sensing so that it can be integrated in a set of networked LED light bulbs. EyeLight forms a mesh of virtual light barriers among nearby light bulbs to sense human presence as they move across the room. Exploiting light provides attractive properties. Due to its nanometer wavelength it is highly sensitive to small motion and objects when compared to RF waves. Also, unlike most RF techniques, light does not suffer from RF interference and cannot penetrate through walls, which preserves privacy and makes it easier

to determine in which room an activity occurred.

Contrary to conventional light barriers, however, no direct line-of-sight is needed—the system exploits opportunistic reflections in the environment (e.g., shadows and reflections off the floor). Indirect tracking of users based on their shadows, enlarges the system’s operation range, compared to line-of-sight based solutions like PIRs. This allows covering a space with fewer sensors and provides more freedom in deployment locations, making it easier to reuse infrastructure that already exists (for example, recessed can lighting where power is available but, due to the recessed location, line-of-sight may not exist to the entire space). Such reuse allows for building-scale motion tracking and activity sensing with little installation overhead (no additional building wiring is needed).

The prototype design makes use of the trend of LED light bulbs increasingly containing electronics and having access to plentiful power. Light bulbs are integrated with photosensors and networked to coordinate signaling and to upload sensor data for processing. We design barrier crossing detection as well as occupancy and activity classification algorithms based on sensed changes in the reflected light levels, for example, due to a shadow. This work significantly extends prior work [10] by 1) using dual purpose signaling light (illumination without causing flicker to the eyes while sending the signature of the node), 2) a room-scale prototype with localization and activity recognition, as well as 3) enhancing sensitivity to operate on different reflective surfaces and longer sensing distances (up to 3 meters).

In summary, the major contributions of this paper are as follows:

- exploring the feasibility of creating opportunistic meshes of virtual light barriers between modified light bulbs by exploiting reflections off room surfaces.
- proposing a sensitive photoreceiver design for lamp-based light barriers that can detect light reflected from different room materials, including dark floor carpet.
- designing light-based occupancy tracking and room activity recognition algorithms and exploring their potential when deployed across a room’s ceiling lighting system.
- designing and implementing a room-scale prototype system and evaluating EyeLight in terms of localization accuracy, estimating occupancy, and recognizing different room activities based on 28.5 hours of recorded data.

## II. BACKGROUND AND RELATED WORK

Visible light sensing can be implemented directly in illumination systems. Adoption of LED lighting is growing rapidly [1] due to their 75% lower energy consumption and 25 times longer lifetime than incandescent lighting. LEDs can also be switched faster than incandescent and fluorescent light sources, which allows rapid signaling with light sources and enables novel applications [2]. Given the presence of solid state devices and power converting circuits (AC to DC) in LED light bulbs, it has also become easier to integrate additional electronics in such devices, particularly since power

is plentiful. To be acceptable, signaling between lights usually has to be imperceptible for human observers.

**Human light perception.** Imperceptible signaling is possible because human eyes respond slower than photodiodes to light changes. The *critical flicker frequency (CFF)* [13], typically 100Hz, defines the frequency beyond which our eyes cannot perceive time-variant light fluctuation and see only its average luminance. This effect is similar to a low pass filter with the CFF as cut-off frequency. While the exact frequency depends on other factors (such as light intensity, color contrasts, etc.), sufficiently fast signaling can surpass the flicker perception of human eyes, yet still remain detectable by photosensor front-ends.

Our eyes also perceive light intensity logarithmically, instead of relatively linearly like photosensors. Therefore, a small change of light intensity that is perceivable in a dark room can be invisible in a brighter room. A photosensor calibrated for this range of light levels can easily detect such differences, however.

**Existing passive sensing techniques.** A major approach to occupancy sensing is using RF signal measurements, based on RSSI ([6], [11]) or time-of-flight [8]. Cameras are also used for monitoring people indoors, but they raise privacy concerns [7]. Other approaches, including Capacitance [22] and Pressure [21] require sensors on the floor, which is not practical for installation in several cases.

Light, both visible and infrared, has long been used for motion detection. Light barriers or curtains [3], [4], for example, detect when a light beam between a source and a photosensor is blocked by a moving object. Since light beams can be easily focused through lenses, they allow more precise movement detection than radiofrequency sensing. To ease deployment, retro-reflective sensors package the light source and sensor into a single device but this usually requires a retroreflector that is carefully aligned to reflect the light back to the sensor.

Visible Light ([15], [20]), an emerging short range communication technology, has been recently explored for indoor localization applications, thanks to the growing use of LED bulbs. More recent works [16], [25] explored the use of ceiling lights in the visible light spectrum to track people indoor. However, either the photosensors are deployed on the floor to achieve line-of-sight to the ceiling lights, which significantly complicates the deployment, or the LEDs are forward biased to function as light sensors, which leads to lower sensitivity and small coverage in the line-of-sight area.

**Challenges in reflective light sensing.** Is it possible to achieve both large coverage and ease of deployment by forming a mesh of opportunistic reflective light barriers?. Allowing for indirect, reflective light sensing could extend the sensing range, since movement can be detected not only directly in line-of-sight of a sensor but also anywhere along the longer reflected path of a light signal. Eliminating the line-of-sight constraint also provides more freedom in placing the lights and sensor. In particular, this approach would allow integrating all necessary components into light bulbs, which would significantly simplify the deployment process: the system could be

installed by simply changing light bulbs. Note also, that power requirements of the added electronics are met by the power source to the LED light and does not require any battery or additional wiring.

This approach introduces several challenges, however. *First*, the detector now has to recognize much weaker light levels due to two reasons: 1) received light power decreases proportional to square of the distance and reflected paths tend to be longer (for example, the distance with a floor reflection to an adjacent ceiling light is more than double compared to the distance with photosensors directly on the floor), and 2) most typical room surfaces absorb or diffuse a substantial part of the light (e.g. a dark carpet), thus the incident light power on the photodiode is reduced. *Second*, the reflected paths are less well defined. The exact path depends on the position and shape of objects in the space and it is possible that the light reaches the photosensor along multiple paths (akin to radio multipath effects). Motion tracking, occupancy estimation, and activity detection algorithms have to be robust to such effects. *Third*, the receiver should be able to distinguish light from different sources. In addition, any signaling technique used for this purpose should remain imperceptible and not detract from the illumination function of light bulbs.

A common method for detecting a weak signal is a correlation detector with a known pseudorandom number (PRN) sequence. This effectively spreads the signal bandwidth leading to a significantly enhanced signal to noise ratio. Applying this to EyeLight is challenging, however. First, achieving high processing gains requires long PRN sequences<sup>1</sup>. Given the limited modulation rate of high power lighting LEDs, these sequences would take seconds to minutes to transmit, which is longer than the duration of human movement events that we seek to detect. Second, transmitting continuous PRN sequences with on-off keying would halve the brightness of the ceiling lights, since one can expect equal number of on and off symbols. Third, as a result of the spectrum spreading property, PRN sequences introduce low frequency components, which increases the chance of flicker for human eyes.

### III. EYELIGHT DESIGN

EyeLight realizes an opportunistic mesh of reflected light barriers through synchronized signaling from networked transmitters and a pulse-based power measurement technique based on sensitive receiver hardware. It relies on modified LED light bulbs to transmit modulated light and contains sensitive photodetectors to detect light signals. It coordinates signaling among light sources so that a virtual light barrier can be established between nearby pairs of lights without interference from other participating light sources. These light barriers are opportunistic since the light needs to reflect off surfaces in the environment to reach the photodetector on an adjacent light bulb. The key rationale for integrating both signaling and sensing components in light bulbs is that it reduces installation

<sup>1</sup>For example, GPS system uses 1023-bit PRN sequence which repeats itself every 1ms.

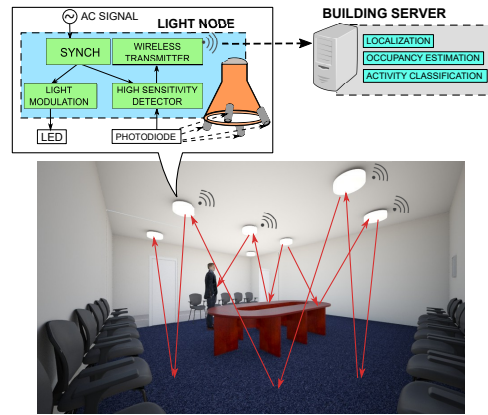


Fig. 1: Overview diagram of components in EyeLight.

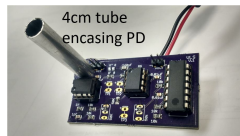
and maintenance costs, as power is already available at the lamps.

It addresses the challenge of invisible modulation of LED light bulbs together with self-interference free detection sensitive enough to measure weak reflections through a synchronous, pulse-based power measurement technique. Bulbs emit a periodic pulse, which is short enough to remain imperceptible, meaning it does not noticeably affect brightness of the light and does not cause flicker. Receivers measure the signal power of the pulse and compare it to the overall light level to track movement and changes in the room.

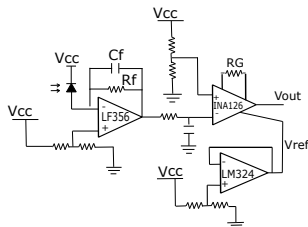
The light nodes have wireless connectivity to report their measurements to a server, where tracking and activity detection algorithms process the datastream to monitor the movements and activities of occupants. We assume that light bulbs can be mapped with their location in the room during installation. Self-localization algorithms may also be possible. Fig. 1 shows an overview of the components in EyeLight.

**Transmitted Signal.** The transmitted signal should allow the receiver to separate light emitted by one specific transmitter from other ambient light sources, while remaining imperceptible to the human eye. In theory, this can be achieved with straightforward ON-OFF signaling. Since flicker perception depends on frequency, this raises the question of whether the high power LEDs used in light bulbs can be switched fast enough to remain imperceptible. We measured the rise and fall time of an off-the-shelf LED bulb (Ecosmart 65W BR30) and observed that the lamp takes about 0.1ms to rise to 90% of its peak intensity and a shorter time to fall. This shows that the light bulbs are fast enough for ON-OFF signaling without introducing flicker to human eyes (previous research [13] showed that the critical flicker frequency of human eyes when perceiving a strong single light source is only about 100Hz).

In addition to eliminating flicker, the signal also should not significantly affect the overall illumination level. We therefore use periodic signaling, which only occurs in a short slot out of a longer cycle. When ceiling lights are used to illuminate the space, the light would briefly switch off during its slot, while remaining on during the rest of a cycle. This design reduces the lamps' brightness by only a negligible amount. Conversely, when lights are off, the lamps could briefly switch on during



(a) Fabricated Receiver.



(b) Receiver Circuit

Fig. 2: Receiver

their slot to signal. Our implementation focuses on the former. Supporting both modes would require additional calibration of receiver sensitivity.

**Receiver.** Sensing reflected light off the floor with photosensors deployed on the ceiling is a challenging task. The photosensor frontend needs a high sensitivity to receive weak light and fast response time to detect the modulated signal. These requirements are usually at odds with each other. We achieve these requirements by carefully designing a receiver circuit combining several components (Fig. 2b). Since we require a fast light sensor to detect short pulse (under 1ms) from the transmitter, we use a photodiode as our sensor. The weak current generated by the photodiode is amplified through a Transimpedance Amplifier. The amplifier acts as the current-to-voltage converter—it converts and amplifies the photocurrent generated by the photodiode to a voltage that can be read out. The amplifying gain of the TIA is set by the feedback resistor  $R_F$  following:  $V_{out}/I_P = -R_F$ .

Compared to a simple detector (a photodiode in series with a resistor  $R$ ), the transimpedance amplifier has much faster response time than the time constant  $R_F * C_d$  (with  $C_d$  is the internal capacitor of the photodiode). Therefore, we can use a larger value of  $R_F$  to increase the gain while maintaining fast response at the front end. However, the value of the feedback resistor cannot be arbitrarily large since it is limited by two factors: large Johnson thermal noise ( $v_n = \sqrt{4k_B T R(V)}$ ) can reduce SNR of the frontend, and low input rolloff frequency ( $f_{RCin} = \frac{1}{2R_F C_{in}}$ ) can limit our operating frequency. To further boost the gain, we use a second stage amplifier: an instrumentation amplifier (INA126). The output of the amplifier is given by,

$$V_o = G(V_+ - V_-) + V_{Ref}$$

where  $V_{Ref}$  is a reference voltage being fed to the instrumentation amplifier, and  $G$  is a controllable gain. One can consider the two inputs to the INA126 as output voltages from two arms of a Wheatstone bridge [10], whose difference we seek to amplify. The negative input  $V_-$  is fed with the output of the TIA, while the positive input  $V_+$  is fed with a constant voltage from a voltage divider. Note that  $G$  and  $V_+$  are two controllable factors that help the receiver adapt to different light levels.

**Multiple Transmitters and Receivers.** The previous two sections describe how a single pair of transmitter and receiver can communicate through reflected light on the floor. When

multiple transmitters are in the room, each light node needs its own identification—when the sensing module detects a light level change because of a shadow, it needs to recognize which light source created that shadow. Therefore, each LED bulb needs a mechanism to send its own signature. This can be done in the frequency domain, as in [16], or time domain. We choose the time domain because of its simplicity when combined with synchronization from the common AC power signal, which our design assumes. As in other prior work [17], the main idea is that each light fixture chooses its own time slot, during which it signals.

For the time-slot based mechanism to work, the clocks of all light nodes need to be synchronized. We implement this by using the common 60Hz AC signal available from the mains power [18]. Recall that a key motivation for incorporating signaling and sensing into light bulbs was the easy availability of power. We therefore also assume a common AC signal for synchronization. Each zero-crossing event of the mains power signal marks the start of a *cycle* for EyeLight, making the cycle length half the period of the AC signal (about 8ms).

Given  $n$  light bulbs that can potentially observe signals from each other, the system requires  $n$  timeslots to uniquely assign a slot to each lamp, which lets the receiver identify the signaling lamp based on the current time. Note that, as in wireless systems, spatial reuse is possible and walls that block light make the reuse of slots across different lamps in a building even easier. This keeps the total number of required time slots relatively small. The maximum number of timeslots that can be supported is determined by the cycle length and the lower slot duration bound derived from the LED rise time.

Besides signaling, each node also looks for signal from other nodes through multiple receivers co-located with the LED lamp. The photosensors point to different directions to detecting signal from surrounding light nodes. For the sampling scheme, we employ a Round-Robin approach to maximize the number of samples per cycle: in each cycle, we let only one photosensor sample the light level in its view, then move to the next photosensors. This ensures each sensor has high enough sampling rate for detecting the fast signal from other nodes.

Fig. 3 shows an example of received light power at one receiver over consecutive cycles. This receiver is on node 2, so it observes a big dip in the second timeslot when node 2 signals. It also observes a smaller dip in the first timeslot, when the adjacent node 1 does signaling. This dip shows the effectiveness of our receiver design to sense weak reflected signals off the floor from an adjacent node.

#### IV. TRACKING ALGORITHMS

The photodiode in each sensor converts the incident radiant energy  $P$  to the output photocurrent  $I_p$ , making our sensor a light power measurement device. In essence, our tracking algorithms utilize signal power measurements over time, and compare them with the baseline light power level when the room is unoccupied. To improve the confidence of our localization, we introduce two methods, *Spike algorithm*

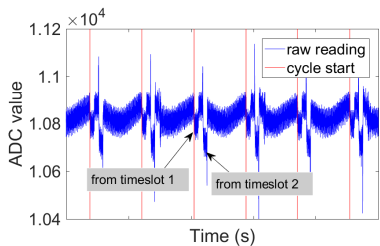


Fig. 3: Raw readings from one receiver.

for coarse-grained localization and *Delta algorithm* for fine-grained localization.

The first method measures if there is any change in received light power, which is caused by movement events surrounding the light node position. We detect this change by continuously taking average received power over an entire cycle for each sensor and using a threshold-based detection to detect when this average power deviates far away from base light level (when the room is empty). This approach, which we call *Spike algorithm*, only tracks movement at a coarse-level—it can only detect if there is a movement event in an area surrounding the spot on the floor a receiver is monitoring.

The second method aims at fine-grained level tracking—it determines whether a change occurred on a specific transmitter-receiver link. With multiple light nodes covering a room and each carrying several receivers, we can effectively create an opportunistic mesh of virtual light barriers to detect when a subject is passing by. Since each light source in the interference domain signals in a unique time slot, receivers can simply check for the presence of the ON-OFF signal in a particular time slot. If the signal can be detected the virtual light barrier is connected, otherwise it is interrupted. This technique is agnostic to most changes in ambient light level that can occur. Over time, the system can then monitor changes in the status of each link.

While the concept is intuitive, its implementation is challenging due to the complex light propagation environment. The system uses reflections off random surfaces rather than direct illumination or a special reflector as in a retro-reflective light barrier. This means that the light level change when the virtual light barrier is crossed can be small and it tends to differ for every pair of lamps. Moreover, in contrast to conventional light barriers, the illuminating signals are more diffuse and the field of view of the sensor is wider to cover a larger area of interest. In addition, multi-path can exist. This means that signals are often only partially blocked when the barrier is crossed.

To address this challenge, EyeLight employs a delta technique. For a given transmitter-receiver link, it measures the delta change in received signal power when the ON-OFF transition occurs and compares it with a delta obtained under reference conditions (i.e., an occupied room). The signal power delta effectively captures how much light from the signaling transmitter is reaching the sensor. It subtracts out all light from other sources, assuming it remains constant over the duration of one slot. If the measured delta significantly deviates from the reference delta, it means that a change between the

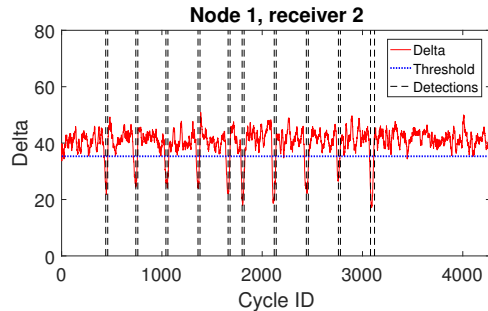


Fig. 4: Virtual light barrier crossing detection.

transmitter and receiver has occurred.

More precisely, let  $P_{i,ON}^{jk}$  and  $P_{i,OFF}^{jk}$  denote the mean power measured by the  $k$ -th sensor on node  $j$  while node  $i$  is in the ON and OFF phase of its signaling, respectively. We define the delta as  $\Delta_i^{jk} = P_{i,ON}^{jk} - P_{i,OFF}^{jk}$ .

Note that both the terms effectively sum all light power reached at the sensor  $k$ , including both the power from ambient light (natural light and illumination from lamps other than  $i$ ) and signaling light power received from lamp  $i$ . That is  $P_i^{jk} = P_{ambient}^{jk} + P_{i,received}^{jk}$ . During OFF phase of lamp  $i$ ,  $P_{i,received}^{jk}$  becomes zero and assuming no change in ambient lighting between ON and OFF phases, it follows that  $\Delta_i^{jk} = P_{i,received,ON}^{jk}$ . This means *the delta value is effectively the light power reflected from node  $i$  to sensor  $j_k$  during the ON phase of node  $i$* . When a person crosses the link between node  $i$  and  $j$ , the person can either block light or reflect more light from node  $i$  to receiver  $j_k$ , depending on the exact position and the reflectivity of the person's hair, skin and clothes. In either case, that causes  $P_{i,received,ON}^{jk}$ , and in effect  $\Delta_i^{jk}$ , to deviate from the normal level.

This observation becomes the key for our light barrier crossing detection method called *Delta algorithm* (Algorithm 1). Going back to the example of receiver  $j_k$ , in each cycle, we calculate the term  $\Delta_i^{jk}$  as described above, then check if this term exceeds a preset threshold range. To reduce noise on the series of calculated delta values, we first apply Hampel filtering to remove outliers and then a low pass filter to smooth the signal. The algorithm then uses a windowing approach (set to 1s) and outputs a detection when the majority of delta values in the window exceed the threshold. We set the threshold based on the mean and the standard deviation of the delta values in the baseline dataset (when the room is unoccupied). (For our prototype, we empirically choose threshold to be  $baseDelta \pm 2 * baseStd$ ). Fig. 4 illustrates one output example of the delta detection algorithm, where receiver 2 on node 1 points to node 2's direction, and a person passes 10 times the light barrier between node 1 and 2.

Given detections from either the Spike algorithm and Delta algorithm, we seek to infer the location of the person. For *Spike algorithm*, based on detections of a user or her shadow in the field of view of different receivers, EyeLight derives the user location based on the positions that these receivers are pointing to. We assign a weight for each receiver based on the magnitude of the deviation of the received light power from

**Algorithm 1:** Delta algorithm - light barrier crossing detection

---

**Input :** readings from node  $j_k$ ,  $baseDeltas$ ,  $baseSTD$   
**Output:** events

```

1 while next cycle exists do
2   cycle = getNextCycle()
3   for  $i = 1 \rightarrow numOfNodes$  do
4      $\Delta_i^{j_k} = P_{i,ON}^{j_k} - P_{i,OFF}^{j_k}$ 
5     Update  $W_i^{j_k}$  - running series of  $\Delta_i^{j_k}$ 
6     hampelfilter( $W_i^{j_k}$ )
7     lowpassfilter( $W_i^{j_k}$ )
8     if  $|\Delta_i^{j_k} - baseDeltas_i^{j_k}| > 2 * baseSTD_i^{j_k}$  then
9       increase count( $events_i^{j_k}$ )
10    end
11    if end of 1-sec window then
12      if (count( $events_i^{j_k}$ ) > window / 2) then
13         $detection_i^{j_k} = True$ 
14      end
15      count( $events_i^{j_k}$ ) = 0
16    end
17  end
18 end

```

---

the baseline level. The final location of the user is estimated as the weighted average of the locations to which the receivers are pointing to. For the *Delta algorithm*, we estimate the location of the user to be the center point between the transmitter and the location the receiver is pointing to.

Note that *Spike algorithm* and *Delta algorithm* compliment each other. The Spike algorithm provides better coverage (any movement in an area surrounding the receiver would be detected) but its location estimation is coarse-grained. In contrast, the Delta algorithm easily pinpoints which transmitter-receiver link the person crosses, but it loses track of a person that does not cross a light barrier link. To obtain both large coverage and fine-grained localization, one can combine the results from both algorithms, for example, by calculating the centroid of their estimated locations.

## V. ROOM ACTIVITY AND OCCUPANCY RECOGNITION

In this section, we introduce the room activity recognition and occupancy classification module. The study focuses on a conference room, with activities and occupancy levels categorized as in Table I. This module uses a supervised machine learning approach based on a feature vector of light power measurements. For other types of rooms, our activity classifier needs to be trained separately to classify different set of activities that commonly happen in these rooms.

The features to be used have to cover all the room's different activity spots, thanks to the non-LOS nature of shadow based tracking. Based on our hypothesis, detecting the room's occupancy and different activities can be inferred from the sources of movements and light settings at different locations. For example, during a presentation activity, the ambient light is usually dimmed and most light received is coming from the projector. One can think of using the delta values and base light level readings during OFF phase of the transmitter

TABLE I: Room activity and occupancy categories

Activity		Occupancy	
Index	Room Activity	Human Count	Category
0	Empty Room	0	Empty Room
1	Sitting at/near Table	1	Single Person
2	Whiteboard Discussion	2-3	Few People
3	Projector Presentation	> 3	Many People
4	Single Person Rehearsing		
5	Conducting Experiments		

for the feature vectors. However, limiting the features to only these two values might cause losing information needed for the classification. Also, the effectiveness of these features depends directly on the base light level, that may change from time to time. Therefore, to capture the temporal and spatial variability of light settings, we use the readings from all the receivers in the room; values for each receiver are 12 average readings of 6 timeslots (including ON and OFF phases). We include the readings from all the time slots since this enables our system to distinguish the source of the lights from multiple directions. The readings are averaged over a span of time window  $w$ . We choose  $w$  to be long enough to capture the different activities and movements by users indoors. Since humans walk on average 1.4 m/s [19], we vary this time window from a second to a minute long. We only report the time window that maximizes the classification accuracy.

Our activity and count recognition approaches uses ensemble learning, specifically AdaBoost.M2 [9]. In Adaboost, the classification results of other learning algorithms ('weak learners') are combined into a weighted sum that represents the final output of the boosted classifier. AdaBoost is able to tweak adaptively the weak learners without prior knowledge about their performance. We use regularized linear discriminant analysis (LDA) learners as weak learners. We train the room activity and occupancy ensemble classifiers with the feature vectors labeled with the activity index and occupancy category label, respectively.

## VI. EYELIGHT PROTOTYPE AND TESTBED

In our prototype, we use an off-the-shelf Ecosmart 65W BR30 LED bulb as the transmitter for each light node. This light bulb contains an AC-to-DC module to provide DC power source to a series of LED chips. For our experiments, we remove this AC-to-DC module and feed 40V DC source directly from a DC power supply to the LED chips. We use a microcontroller (MSP432) to control a power MOSFET (IRFL520) as a switch to drive much larger current needed for the LED lamp. For *timeslot assignment*, to support 6 nodes, we divide each cycle (8ms) into 6 even timeslots.

In the transimpedance amplifier, we use the LF356 op-amp, which has low input noise voltage and suitable for photosensor amplifier task. The feedback resistor is 10M $\Omega$  to maximize the transimpedance gain. In the later stage, further amplification is achieved by using INA126, an instrumentation amplifier with low noise characteristics.

We use TI MSP432 Launchpad to control both transmitter and receiver operations. The MSP432 Launchpad also offloads

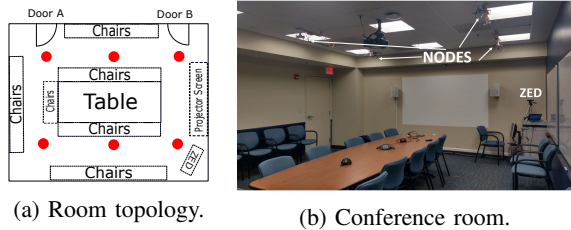


Fig. 5: EyeLight testbed. There are 6 light nodes with distance between adjacent pair is 2.5m. The room has a central table, a number of chairs, and a projector screen.

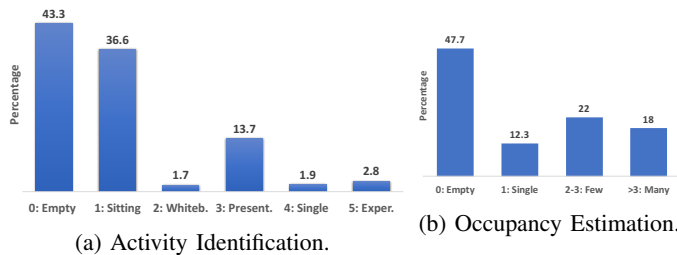


Fig. 6: The distribution of different activities and occupancy categories in the dataset.

data measurement through Wi-Fi to our processing server with the help of a TI CC3100 BoosterPack.

We built 6 light nodes and placed them inside a conference room (size  $7.5 \times 6m^2$ , ceiling height  $2.74m$ ), as shown in Fig. 5. All circuit components for each light node were placed on a woodplank together with the LED light bulb. We placed 4 receivers around each LED bulb, pointing to different directions; each photodiode is titled  $\theta = 10^0$  compared to the vertical line. This placement of photodiodes increases the number of virtual light barriers in the room to detect human presence. To construct groundtruth, we placed a ZED depth camera [5] in the corner of the room. The camera records videos of the room with depth information, and these videos are later manually processed to rebuild the positions of all persons inside the room.

VII. EYELIGHT EVALUATION

We collected data using our testbed in a conference room for 5 days over multiple weeks. For each day, we recorded data during normal working hours, the total number of hours recorded being 28.5 hours. Different users entered the room, including visitors, staff, faculty and students. Different lighting settings and different chairs organizations have been conducted during these days. We collected the base light level for the Spike and Delta algorithms at the beginning of each day.

A. Light barrier crossing detection accuracy

The output of the Delta detection algorithm for each photoreceiver is a binary detection: for each second, whether there is shadow casted by the adjacent node on the floor where the receiver is looking at. To evaluate the accuracy of our Delta detection algorithm, we conduct an experiment

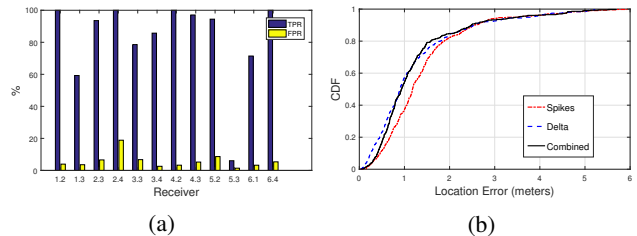


Fig. 7: (a) TPR and TNR of delta detection algorithm. (b) CDF of localization error.

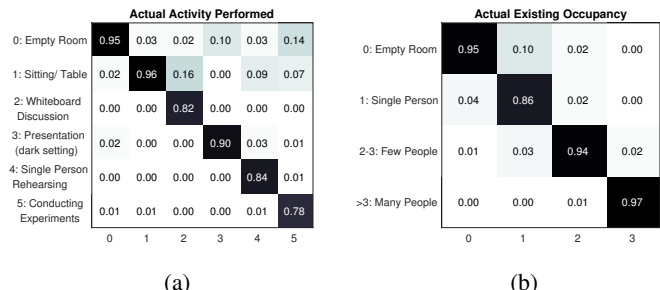


Fig. 8: Confusion matrix for 28.5-hour experiment in a conference room. (a) Activity identification. (b) Occupancy estimation.

in which several test subjects walk in the room across all the lamps. Fig. 7a shows the True Positive Rate (TPR) and False Positive Rate (FPR) of the delta detection algorithm for different photoreceivers. TPR is the ratio of the correctly detected events over the total number of proximity events, and FPR is the ratio of the incorrectly detected events over the total number of testing cases when no person is in the vicinity of a sensor. The receivers in the figure are the ones pointing to an adjacent light bulb. The average TPR across all receivers is 82.17% and the average FPR is 5.77%. Among all receivers, only receiver 5.3 has low TPR (6%). Given our conference room has dark carpet with low reflected light, the TPR and FPR value reported here are reasonably good. Also, this is the performance for each single receiver; we expect that by combining multiple receivers together, the accuracy of the whole system would be higher.

B. Localization error

Fig. 7b shows the localization error for single-person tracking scenarios, using three different methods: using only spikes detection, using only delta detection, and combined. Delta detection shows lower localization error (median 0.89m and 90 percentile of 2.5m) than spikes detection (median 1.18m and 90 percentile of 2.56m). However, the spikes detection is achieving this localization error while covering 94% of the time in which the user is inside the room compared to 69% for the delta detection. It is clear that there is a tradeoff here between the coverage and localization accuracy. Therefore, we also propose the combined version of the two algorithms, which achieves a 0.94m median error and better coverage rate than the delta detection.

### C. Room Activity Recognition and Occupancy Estimation

We evaluate our room activity recognition classifier by 10-fold cross validation over the whole collected dataset using random partitioning. Each feature vector represents the average readings over a 5-second period, which maximizes the classification accuracy. Fig. 8a shows the confusion matrix for the classification results of our activity recognition classifier. Each column represents the actual activity performed by the user and each row shows the activity as classified by our system. The overall classification accuracy is 93.78%; however, if we break down the TPR for each activity, we can see the performance degrades for categories 2: whiteboard discussion, 4: single rehearsal and 5: conducting experiments. These activities represent a small fraction of the collected data as presented in Fig. 6a, and therefore, the classifier likely has not enough data to accurately capture the true model of these classes. Also, class 3, presentation in the dark, is easily misidentified as class 0, empty room, since the room is almost dark, and during presentation there are not many movements to capture. However, we expect collecting more data specially for these classes will decrease the classification error.

EyeLight is able to distinguish 4 classes of occupancy of a room, by classifying the readings coming from all the nodes inside. Each feature vector represents the average readings over a 10-second period, which maximizes the classification accuracy. We used the same evaluation procedure of the activity recognition classifier (10-fold cross validation). Fig. 8b shows the confusion matrix for occupancy estimation classifier. The overall accuracy of the classifier is 93.7%, while the TPR for single person class is lowest among all the classes with 86%. A single person staying in a conference room is not a common event, so the dataset for this class is not enough. Detecting a single person is thus more challenging than multiple persons specifically, since the collected data for single-person class is also the lowest among the four classes as in Fig. 6b. Moreover, a single person induces low effect on the light especially when not moving (e.g., sitting near the table and working with on a laptop). Therefore, we moved from five-second feature vectors, as in the activity recognition, to a ten-second feature vector in order to capture more of these rare movements for a single user. Again, we expect that collecting more data for this class would improve the classification accuracy.

### D. Microbenchmark experiments

**Distance between nodes.** We increase the distance between the two nodes and measure the delta values received in one receiver for each distance between two nodes (Fig. 9a). As the distance between two nodes increases, the delta value becomes smaller; starting from 3.5 meters, this delta is too small to distinguish from noise, rendering EyeLight ineffective to use.

**Number of nodes.** We measure the localization median error of two algorithms (Spikes and Delta) with reducing number of nodes to cover our conference room (Fig. 9b). Note that there is no data for single node case of the Delta algorithm detection, since it needs at least a communication link between

two nodes. As expected, the location accuracy reduces as the number of nodes decreases, because either the number of guarded locations (for Spike detection) or the number of virtual light barriers (for Delta detection) decreases.

**Ambient light.** We test different ambient light settings in our conference room: no ambient light, only ceiling lights turned on, only side lights turned on, both ceiling lights and side lights turned on. The mean and standard deviation of delta values for each light setting over a period of time is shown in Fig. 9c. For each ambient light setting, the standard deviation is small, allows the delta algorithm to work efficiently. However, the mean value of deltas slightly differs between light settings, suggesting that the system might need to calibrate for several times a day, when the ambient light setting is changed.

**Different types of carpets.** Another factor that affects the efficiency of the delta-based virtual light barrier crossing detector is the reflectivity of the floor carpet materials. The carpet inside our conference room is dark, and thus reflects less light. To see the applicability of our detection algorithm on other types of carpets, we tested a light node facing different types of carpets (Fig. 9e) and compute the delta values (Fig. 9d). As can be seen, two other carpets have brighter surface, giving much larger delta values. Therefore, we believe EyeLight is also suitable to work with other room carpet, with even better performance. For other floor types, such as tiles, wood, due smoother surface, they reflect light even better than carpets, thus are also applicable in EyeLight.

**Lamp shade.** In all previous experiments, we tested with commercial light bulbs without lamp shades. To show the effect of lamp shade on the transmitted signal, we compared the average delta values for lamps with and without lampshade (Fig. 9f). The result shows that with lamp shade on, the average delta value actually increases. One might think that lampshade would reduce the intensity of the light from the transmitter, weakening received light power at the receiver. In fact, however, the lamp shade distributes light more evenly over the floor area under the lamp, thus improve the sensitivity of the receivers looking at different spots on the floor.

## VIII. DISCUSSION AND CONCLUSION

We proposed a device-free indoor tracking, occupancy estimation and activity recognition system that can be integrated in light-bulbs. The key idea is to create a mesh of reflective virtual light barriers across networked light bulbs to detect occupant movement. We found that our high-sensitivity photo-sensing circuit can detect minute light changes (shadows) even on dark carpeting, and that a time division pulse signaling scheme allows differentiating the light nodes causing shadows on the floor. With our 45  $m^2$  conference room prototype system with 6 light bulbs each carrying 4 receivers, we further found that the sensing system can achieve a 0.89m median localization error as well as 93.7% and 93.78% occupancy and activity classification accuracy, respectively.

Our current system still has several limitations that could be addressed in future work. *First*, EyeLight requires more than



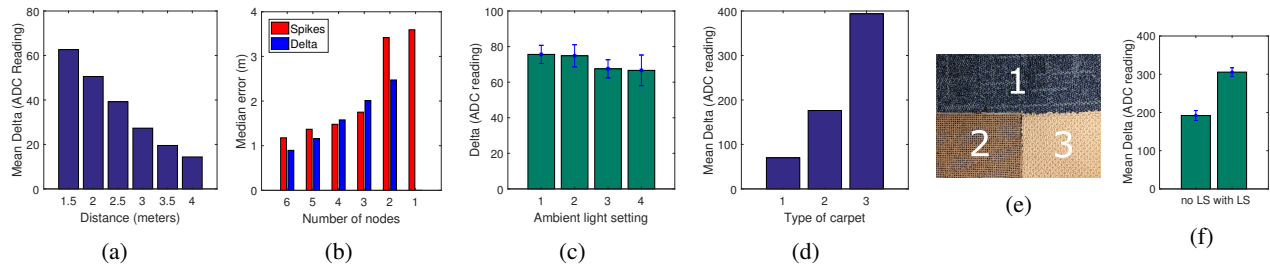


Fig. 9: (a) Delta values for different distance between two nodes. (b) Location median error for different number of nodes. (c) Delta values for different ambient light settings. (d) Delta values for different types of floor carpets. (e) Types of carpet in (d). (f) Effect of lamp shade.

one lamp per room for fine-grained user tracking. Fortunately, the small size of LED lights makes it easier to add additional lights in rooms. *Second*, EyeLight so far focuses on tracking a single person per room. It could track multiple persons as long as they cross different virtual light barriers, while multiple persons walking together leads to mixed shadows. *Third*, EyeLight needs to adapt to different light settings, such as different times of the day, rooms with outdoor light passing through windows. Currently our prototype works in a conference room without windows, where measured illuminance of light reflected from the floor is under 5 lux. In a room with outdoor light entering through windows, the current receivers saturate. However, techniques like Adaptive Gain Control, as used in other systems dealing with high dynamic range, can be added to EyeLight to improve its robustness. An adaptive system is also needed to keep track of the change of the baseline light level. We leave such designs for future work.

## IX. ACKNOWLEDGMENT

This work was supported in part by the US National Science Foundation (NSF) under grants CNS-1409811 and CNS-1329939.

## REFERENCES

- [1] <http://www.energy.gov/energysaver/led-lighting>.
- [2] <http://www.ledsmagazine.com/articles/2005/01/benefits-and-drawbacks-of-leds.html>.
- [3] <http://ab.rockwellautomation.com/Sensors-Switches/Operator-Safety/Light-Curtain>.
- [4] [https://www.pepperl-fuchs.com/global/en/classid\\_4294.htm](https://www.pepperl-fuchs.com/global/en/classid_4294.htm).
- [5] <https://www.stereolabs.com/>.
- [6] P. Bahl and V. N. Padmanabhan. Radar: an in-building rf-based user location and tracking system. In *Proc. IEEE INFOCOM 2000 Conf. on Comput. Commun. 19th Annu. Joint Conf. IEEE Comput. and Commun. Soc.*, volume 2, pages 775–784 vol.2, 2000.
- [7] K. E. Caine, A. D. Fisk, and W. A. Rogers. Benefits and privacy concerns of a home equipped with a visual sensing system: A perspective from older adults. In *Proc. of the human factors and ergonomics society annual meeting*, volume 50.
- [8] Z. Kabelac F. Adib and D. Katabi. Multi-person localization via rf body reflections. In *12th USENIX Symposium on Networked Systems Design and Implementation (NSDI'15)*, Oakland, CA.
- [9] Y. Freund and R. E. Schapire. A decision-theoretic generalization of on-line learning and an application to boosting. In *European conference on computational learning theory*, pages 23–37. Springer, 1995.
- [10] M. Ibrahim, V. Nguyen, S. Rupavatharam, M. Jawahar, M. Gruteser, and R. Howard. Visible light based activity sensing using ceiling photosensors. In *Proc. of the 3rd Workshop on Visible Light Commun. Syst., VLCS '16*, pages 43–48, New York, NY, USA, 2016. ACM.
- [11] M. Ibrahim, M. and Youssef. CellSense: An accurate energy-efficient gsm positioning system. *IEEE Trans. on Vehicular Technology*, 2012.
- [12] M. Keally, G. Zhou, G. Xing, J. Wu, and A. Pyles. Pbn: Towards practical activity recognition using smartphone-based body sensor networks. In *Proc. of the 9th ACM Conf. on Embedded Networked Sensor Syst.*, pages 246–259. ACM, 2011.
- [13] D.H. Kelly. Sine waves and flicker fusion. *Documenta Ophthalmologica*, 18(1):16–35, 1964.
- [14] J. Lei, X. Ren, and D. Fox. Fine-grained kitchen activity recognition using rgb-d. *UbiComp '12*, pages 208–211. ACM, 2012.
- [15] L. Li, P. Hu, C. Peng, G. Shen, and F. Zhao. Epsilon: A visible light based positioning system. In *11th USENIX Symposium on Networked Systems Design and Implementation (NSDI 14)*, Seattle, WA.
- [16] T. Li, C. An, Z. Tian, A. T. Campbell, and X. Zhou. Human sensing using visible light communication. In *Proc. of the 21st Annu. Int. Conf. on Mobile Computing and Networking, MobiCom '15*, 2015.
- [17] T. Li, Q. Liu, and X. Zhou. Practical human sensing in the light. In *Proc. of the 14th Annu. Int. Conf. on Mobile Syst., Applicat., and Services, MobiSys '16*, pages 71–84, New York, NY, USA, 2016. ACM.
- [18] Z. Li, W. Chen, C. Li, M. Li, Xiang-Yang Li, and Y. Liu. Flight: Clock calibration using fluorescent lighting. In *Proc. of the 18th Annu. Int. Conf. on Mobile Computing and Networking, Mobicom '12*, pages 329–340, New York, NY, USA, 2012. ACM.
- [19] B. J. Mohler, W. B. Thompson, S. H. Creem-Regehr, H. L. Pick, and W. H. Warren. Visual flow influences gait transition speed and preferred walking speed. *Experimental brain research*, 181(2):221–228, 2007.
- [20] V. Nguyen, Y. Tang, A. Ashok, M. Gruteser, K. Dana, W. Hu, E. Wengrowski, and N. Mandayam. High-rate flicker-free screen-camera communication with spatially adaptive embedding. In *IEEE INFOCOM 2016*, pages 1–9, April 2016.
- [21] R. J. Orr and G. D. Abowd. The smart floor: A mechanism for natural user identification and tracking. In *CHI '00 Extended Abstracts on Human Factors in Computing Syst., CHI EA '00*, pages 275–276, New York, NY, USA, 2000. ACM.
- [22] M. Valtonen, J. Maentausta, and J. Vanhala. Tiletrack: Capacitive human tracking using floor tiles. In *2009 IEEE Int. Conf. on Pervasive Computing and Commun.*, pages 1–10, March 2009.
- [23] Yan Wang, Jian Liu, Yingying Chen, Marco Gruteser, Jie Yang, and Hongbo Liu. E-eyes: device-free location-oriented activity identification using fine-grained wifi signatures. In *Proc. of the 20th Annual Int. Conf. on Mobile Computing and Networking*, pages 617–628. ACM, 2014.
- [24] C. R. Wren and E. M. Tapia. Toward scalable activity recognition for sensor networks. In *LoCA*, volume 3987, pages 168–185, 2006.
- [25] Y. Yang, J. Hao, J. Luo, and S. J. Pan. Ceilingsee: Device-free occupancy inference through lighting infrastructure based led sensing. In *Proc. of the 15th Int. Conf. on Pervasive Computing and Commun., Percom '17*. IEEE, 2016.
- [26] J. Yun and Sang-Shin Lee. Human movement detection and identification using pyroelectric infrared sensors. *Sensors*, 14(5):8057–8081, 2014.
- [27] C. Zhang and X. Zhang. Litell: Robust indoor localization using unmodified light fixtures. In *Proc. of the 22nd Annu. Int. Conf. on Mobile Computing and Networking, MobiCom '16*, pages 230–242, New York, NY, USA, 2016. ACM.